

# Oncolytic herpes simplex virus expressing IL-2 controls glioblastoma growth and improves survival

Praveen K Bommareddy <sup>1,2</sup>, Hiroaki Wakimoto <sup>1</sup>, Robert L Martuza,<sup>1</sup>  
Howard L Kaufman <sup>1,3</sup>, Samuel D Rabkin <sup>1</sup>, Dipongkor Saha <sup>4,5</sup>

**To cite:** Bommareddy PK, Wakimoto H, Martuza RL, *et al.* Oncolytic herpes simplex virus expressing IL-2 controls glioblastoma growth and improves survival. *Journal for ImmunoTherapy of Cancer* 2024;**12**:e008880. doi:10.1136/jitc-2024-008880

Accepted 01 March 2024



© Author(s) (or their employer(s)) 2024. Re-use permitted under CC BY-NC. No commercial re-use. See rights and permissions. Published by BMJ.

<sup>1</sup>Department of Neurosurgery, Massachusetts General Hospital and Harvard Medical School, Brain Tumor Research Center, Boston, Massachusetts, USA

<sup>2</sup>Cancer Institute of New Jersey (CINJ), New Brunswick, New Jersey, USA

<sup>3</sup>Department of Surgery, Massachusetts General Hospital, Boston, Massachusetts, USA

<sup>4</sup>Department of Pharmaceutical and Biomedical Sciences, California Northstate University College of Pharmacy, Elk Grove, California, USA

<sup>5</sup>Department of Immunotherapeutics and Biotechnology, Texas Tech University Health Sciences Center School of Pharmacy, Abilene, Texas, USA

## Correspondence to

Dr Dipongkor Saha;  
Dipongkor.Saha@cnsu.edu

## ABSTRACT

**Background** Glioblastoma (GBM), a highly immunosuppressive and often fatal primary brain tumor, lacks effective treatment options. GBMs contain a subpopulation of GBM stem-like cells (GSCs) that play a central role in tumor initiation, progression, and treatment resistance. Oncolytic viruses, especially oncolytic herpes simplex virus (oHSV), replicate selectively in cancer cells and trigger antitumor immunity—a phenomenon termed the “in situ vaccine” effect. Although talimogene laherparepvec (T-VEC), an oHSV armed with granulocyte macrophage-colony stimulating factor (GM-CSF), is Food and Drug Administration (FDA)-approved for melanoma, its use in patients with GBM has not been reported. Interleukin 2 (IL-2) is another established immunotherapy that stimulates T cell growth and orchestrates antitumor responses. IL-2 is FDA-approved for melanoma and renal cell carcinoma but has not been widely evaluated in GBM, and IL-2 treatment is limited by its short half-life, minimal tumor accumulation, and significant systemic toxicity. We hypothesize that local intratumoral expression of IL-2 by an oHSV would avoid the systemic IL-2-related therapeutic drawbacks while simultaneously producing beneficial antitumor immunity.

**Methods** We developed G47Δ-mIL2 (an oHSV expressing IL-2) using the flip-flop HSV BAC system to deliver IL-2 locally within the tumor microenvironment (TME). We then tested its efficacy in orthotopic mouse GBM models (005 GSC, CT-2A, and GL261) and evaluated immune profiles in the treated tumors and spleens by flow cytometry and immunohistochemistry.

**Results** G47Δ-mIL2 significantly prolonged median survival without any observable systemic IL-2-related toxicity in the 005 and CT-2A models but not in the GL261 model due to the non-permissive nature of GL261 cells to HSV infection. The therapeutic activity of G47Δ-mIL2 in the 005 GBM model was associated with increased intratumoral infiltration of CD8<sup>+</sup> T cells, critically dependent on the release of IL-2 within the TME, and CD4<sup>+</sup> T cells as their depletion completely abrogated therapeutic efficacy. The use of anti-PD-1 immune checkpoint blockade did not improve the therapeutic outcome of G47Δ-mIL2.

**Conclusions** Our findings illustrate that G47Δ-mIL2 is efficacious, stimulates antitumor immunity against orthotopic GBM, and may also target GSC. OHSV expressing IL-2 may represent an agent that merits further exploration in patients with GBM.

## WHAT IS ALREADY KNOWN ON THIS TOPIC

⇒ Glioblastoma (GBM) is highly immunosuppressive and contains a subpopulation of GBM stem-like cells (GSCs) associated with drug resistance. While oncolytic herpes simplex virus (oHSV), including the FDA-approved T-VEC, holds promise in cancer immunotherapy, its effectiveness in GBM remains unreported. Similarly, although systemic interleukin-2 (IL-2) cytokine therapy is FDA-approved for cancer, its systemic administration is associated with toxicities.

## WHAT THIS STUDY ADDS

⇒ The study introduces a novel oHSV expressing IL-2 (G47Δ-IL2), aiming to leverage the “in situ vaccine” effect, demonstrating a significant extension of median survival in mice bearing GSC-derived orthotopic tumors without systemic IL-2-related toxicity, and the therapeutic effects hinge on the local release of IL-2, with CD4<sup>+</sup> T cells playing a critical role.

## HOW THIS STUDY MIGHT AFFECT RESEARCH, PRACTICE OR POLICY

⇒ The therapeutic activity of G47Δ-IL2 in stimulating antitumor immunity and targeting GSC-derived tumors suggests its potential as a novel treatment for GBM, warranting further exploration and clinical investigation.

## INTRODUCTION

Glioblastoma (GBM), the most common primary malignant brain tumor, is highly immunosuppressive and has no effective treatments.<sup>1</sup> Even immune checkpoint inhibitor (ICI) immunotherapy has proven ineffective in GBM.<sup>2</sup> Additionally, GBM contains a subpopulation of GBM stem-like cells (GSCs) that play a central role in tumor initiation, progression, maintenance, and recurrence.<sup>3</sup> They self-renew, efficiently form heterogeneous tumors,<sup>4</sup> and exhibit phenotypic and genotypic similarity to primary GBM.<sup>5</sup> Thus, GSCs may be responsible for the high rate of drug resistance seen in GBM and could be important therapeutic targets.



GBM tumor cell lines generated from patient-derived GSCs recapitulate GBM histology in immunodeficient mice,<sup>6</sup> but this model is not suitable for evaluating antitumor immunity. Thus, we developed an immunocompetent mouse GSC-derived (005) orthotopic brain tumor model,<sup>7</sup> which originated from GSCs that were isolated from GBM induced with lentiviral transduction of brains with H-Ras<sup>V12</sup> and activated Akt in Cre-GFAP/p53<sup>+/-</sup> mice.<sup>8</sup> This model recapitulates histological and immunosuppressive features of human GBM,<sup>7-10</sup> such as low immunogenicity,<sup>7,10</sup> high tumorigenicity, invasiveness<sup>7,11</sup> with heterogeneous histopathology,<sup>7</sup> immunosuppressive tumor microenvironment (TME),<sup>7,9,11</sup> and limited responsiveness to ICI.<sup>9,10</sup> Notably, the tumor-infiltrating immune cell profile of 005 tumors resembles that of GBM patients.<sup>12</sup> Like the 005 GBM model, the carcinogen-induced CT-2A GBM model retains GSC-like features,<sup>13-15</sup> immunosuppression,<sup>15</sup> and insensitivity to ICI treatments.<sup>10</sup> Both 005 and CT-2A models, because of their phenotypic similarity to human GBM, are suitable for testing new anti-GBM immunotherapeutics.

Oncolytic viruses (OVs) such as oncolytic herpes simplex virus (oHSV) represent a promising anticancer approach.<sup>16</sup> OHSV selectively replicates in cancer cells (sparing normal cells), including human GSCs,<sup>17</sup> and induces antitumor immunity (ie, *in situ* vaccine effect).<sup>16</sup> An oHSV armed with GM-CSF (T-VEC) is FDA-approved for advanced melanoma.<sup>18</sup> However, the safety and efficacy of T-VEC in GBM patients have not been reported. OHSV G47Δ, designed similarly to T-VEC but lacking GM-CSF expression,<sup>19</sup> is approved in Japan for recurrent GBM.<sup>20</sup> However, G47Δ-Empty (a derivative of G47Δ lacking transgene) produces limited anti-GBM efficacy, as demonstrated in the 005 GSC model.<sup>7</sup> Given the HSV-1 genome can accommodate foreign transgene expression, we sought to develop a G47Δ-based oHSV vector expressing a potent immune stimulatory gene.

Interleukin 2 (IL-2) is a proinflammatory cytokine known for its diverse effects, including stimulating T cell growth and coordinating the immune system's cytotoxic T lymphocyte (CTL)-mediated antitumor response.<sup>21</sup> Given these properties, IL-2 is regarded as a pivotal proinflammatory cytokine in combating cancer, and high-dose IL-2 has received clinical approval for treating advanced renal cell carcinoma and melanoma. Despite FDA approval, systemic IL-2 therapy falls short of delivering anticipated antitumor effects due to its short half-life and low tumor accumulation.<sup>22</sup> Moreover, frequent high-dose systemic IL-2 administration requires intensive patient monitoring and can result in life-threatening toxicities, such as vascular leak syndrome.<sup>23</sup> We hypothesized that IL-2 expression by an oHSV within the TME would avoid systemic IL-2-related therapeutic toxicity while simultaneously producing beneficial antitumor immunity.

Therefore, we used oHSV G47Δ<sup>19</sup> to generate a novel oHSV expressing murine IL-2 (G47Δ-mIL2) for local intratumoral expression of the IL-2. Subsequently, we evaluated anti-GBM efficacy of G47Δ-mIL2 in mouse

GBM models (005 GSC and CT-2A). Our findings demonstrate that G47Δ-mIL2 significantly extends the median survival of mice-bearing 005 GSC- or CT-2A-derived brain tumors. Local release of IL-2 following viral treatment within the 005 tumor is necessary for therapeutic benefit and correlated with increased infiltration of T cells, notably CD8<sup>+</sup> T cells, into the TME. In this model, the therapeutic effects were also dependent on CD4<sup>+</sup> T cells as G47Δ-mIL2 treatment was completely abrogated in the absence of CD4<sup>+</sup> T cells. These results have implications for translation into human clinical trials of GBM.

## METHODS

### Cells and viruses

005 GSCs were grown as neurospheres in serum-free stem cell medium following previously established protocols.<sup>7,10</sup> Mouse CT-2A glioma cells and mouse GL261 cells were grown on plastic in Dulbecco's Modified Eagle Medium (DMEM) supplemented with 10% fetal calf serum. All cultures were maintained at 37°C in 5% CO<sub>2</sub>. Only low-passage single cells, confirmed to be mycoplasma-free (LookOut mycoplasma kit; Sigma), were employed in our experiments.

G47Δ-mIL2 was created using G47Δ, which features deletions in the  $\gamma$ 34.5 and  $\alpha$ 47 genes and an inactivating insertion of LacZ into ICP6,<sup>19</sup> following the established protocol of the flip-flop HSV-BAC system.<sup>24</sup> Briefly, murine IL-2 cDNA, driven by the HSV immediate-early (ie, 4/5) promoter, linked to a mCherry protein via a P2A peptide, that is, mIL2-P2A-mCherry, was inserted into the backbone of oHSV (G47Δ), using the flip-flop HSV-BAC system, in the deleted ICP6 region<sup>24</sup> (figure 1A). G47Δ-mIL2 was grown in Vero cells (purchased from ATCC) after a low multiplicity of infection (MOI) and purified as described in Nguyen *et al.*<sup>25</sup>

### Cytotoxicity assay and fluorescence microscopy

For the cytotoxicity assay, dissociated mouse 005 GSCs were seeded into 96-well cell culture plates, the virus was added at indicated doses immediately after seeding, and cells were incubated for 4 days at 37°C before conducting MTS assays (Promega). Each experiment was independently repeated at least twice and performed in triplicate. Dose-response curves and IC50 values were calculated using Prism 9 software V.9.5.1. For mCherry expression, mouse 005 GSCs (100,000 cells/well) were inoculated with phosphate-buffered saline (PBS) or G47Δ-mIL2 at a MOI of 1.0, incubated at 37°C, and images were captured at 24-hour post-treatment by light/fluorescent microscopy.

### Mouse survival studies

C57BL/6 or athymic mice (7–8 weeks old) were purchased from the National Cancer Institute (Envigo). Dissociated 005 GSCs (2×10<sup>4</sup> cells/mouse), CT-2A cells (1×10<sup>4</sup> cells/mouse), or GL261 cells (3×10<sup>4</sup> cells/mouse) in 3μL of their respective media were implanted into the striatum by stereotactic injection (2.2 mm lateral from Bregma

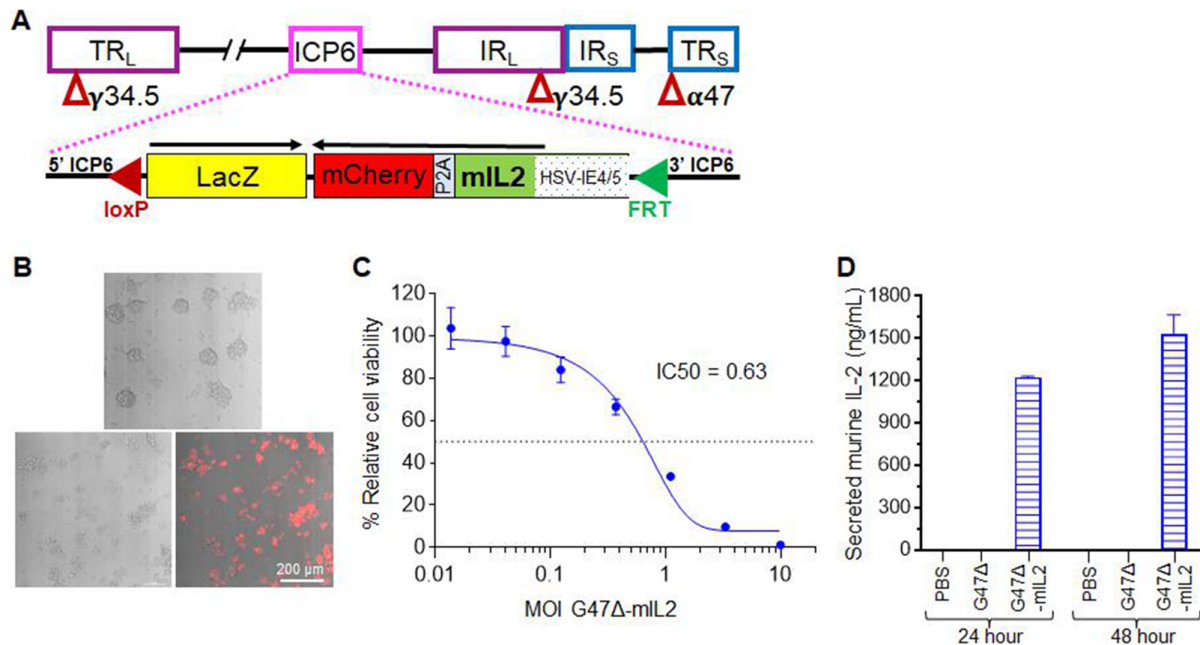


**Figure 1** (A) Construction of G47Δ-mIL2. Murine IL-2 (mIL2) was inserted into the backbone of G47Δ using the flip-flop HSV-BAC system.<sup>24</sup> G47Δ is a third-generation oHSV with deletions in the  $\gamma$ 34.5 and  $\alpha$ 47 genes and an inactivating LacZ insertion into infected cell protein 6 (ICP6).<sup>19</sup> G47Δ-mIL2 contains an insertion of murine IL-2 in the deleted ICP6 region driven by the HSV immediate-early (ie, 4/5) promoter. Murine IL-2 was linked with a bright red monomeric fluorescent protein (mCherry) by a P2A peptide. TR<sub>L</sub> or TR<sub>S</sub>, terminal repeat long or short; IR<sub>L</sub> or IR<sub>S</sub>, internal repeat long or short. (B) G47Δ-mIL2 expresses mCherry monomeric fluorescent red protein. Mouse 005 GSCs were inoculated with PBS or G47Δ-mIL2 at a multiplicity of infection (MOI) of 1.0, incubated at 37°C, and images were captured at 24-hour post-treatment by light/fluorescent microscopy. Upper panel: A phase contrast image of PBS-treated 005 GSC-derived neurospheres; Lower panels: A phase contrast image of G47Δ-mIL2-infected 005 GSCs (lower left) and a merged image showing mCherry expression from G47Δ-mIL2-infected 005 GSCs (lower right). (C) Dose-response curve of G47Δ-mIL2 in mouse 005 GSCs in vitro. 005 GSCs (2000 cells/well) were seeded on a 96-well tissue culture plate. Immediately after plating, 005 GSCs were inoculated with various MOI of G47Δ-mIL2, incubated at 37°C for 96 hours, and relative cell viability was measured by MTS cytotoxicity assay (Promega). The graph represents the mean±SEM of two experiments performed in triplicate. (D) G47Δ-mIL2 secretes murine IL-2. Vero cells were plated on a 6-well tissue culture plate (200 000 cells/well) and incubated for 12 hours at 37°C. Afterward, cells were washed twice with PBS, inoculated with G47Δ or G47Δ-mIL2 with an MOI of 0.1, and incubated for 2 hours at 37°C. Then, the virus inoculum was removed, washed with PBS twice to remove free viral particles, added fresh Vero cell growth medium (containing 1% fetal bovine serum), and incubated at 37°C for 24–48 hours postvirus inoculation and tested for the presence of murine IL-2 by ELISA (Bio-Techne). The data are presented as mean±SEM, and the experiments were performed in duplicate. GSC, GBM stem-like cells; HSV, herpes simplex virus. PBS, phosphate-buffered saline.

and 2.5 mm deep) to establish orthotopic intracranial tumors. On indicated days after tumor implantation, mice were randomly allocated into groups and received a single intratumoral injection of G47Δ-mIL2 (as indicated) or PBS in 2  $\mu$ L at the same stereotaxic coordinates. IL-2 neutralizing antibodies anti-murine IL-2 (anti-mIL-2; clone JES6-1A12; 10 mg/kg followed by 7.5 mg/kg), ICI anti-murine PD-1 antibodies (anti-mPD-1; clone RMP1-14; 10 mg/kg), immune cell depletion antibodies, such as anti-CD4 (clone GK1.5; 10 mg/kg), anti-CD8 (clone 2.43; 10 mg/kg), anti-NK1.1 (clone PK136; 10 mg/kg), or combination of anti-CD8 plus anti-NK1.1 (10 mg/kg each), or control IgGs were obtained from BioXcell and administered intraperitoneally on indicated days after tumor implantation. Mice were followed for neurological symptoms and body weight and euthanized before becoming moribund. Animal caretakers were blinded to the treatment. The presence of the tumor at sacrifice was

evaluated macroscopically or after histological staining of sections.

#### ELISA

Mouse IL-2 was quantified from cell culture supernatants (infected at MOI=0.1), brain supernatants, or mice sera using the Mouse IL-2 Quantikine ELISA kit (M2000) (Bio-Techne, R&D Systems). Each cell culture, tumor homogenate, or serum sample was assessed in duplicate.

#### Multicolor flow cytometry

C57BL/6 mice were intracranially implanted with mouse 005 GSCs. On day 22, these mice were treated intratumorally with either PBS or G47Δ-mIL2 and euthanized on day 29. Brain tumor quadrants were harvested, minced, and single-cell suspensions were prepared as described.<sup>26</sup> The samples were preincubated with purified anti-CD16/32 unconjugated antibodies (clone 93) to block Fc receptors prior to surface staining with fluorochrome-conjugated



anti-mouse monoclonal antibodies against CD45 (clone 30-F11), CD3 (clone 17A2), CD4 (clone GK1.5), CD8a (clone 53-6.7), CD279 (clone 29F.1A12), as well as appropriate isotype control antibodies.<sup>26</sup> Fixable Viability Dye eFluor 506 (eBioscience) was used to stain dead cells. Intracellular FOXP3 and Ki67 staining were performed using color-conjugated anti-mouse FOXP3 (clone MF-14) and anti-mouse Ki-67 (clone 16A8), respectively, following the intracellular staining protocol (eBioscience). All antibodies were purchased from BioLegend. For multicolor FACS staining of spleens and tumor-draining lymph nodes, single-cell suspensions from these organs were prepared<sup>26</sup> and stained as above. Fluorescent minus one (FMO) controls were included.<sup>10</sup> Data were acquired on BD Fortessa and analyzed with FlowJo software V.10.6.1 (Tree Star). The scientific person involved in acquiring and gating the data was blinded to the treatments.

### Immunohistochemistry for tumor-infiltrating immune cells

C57BL/6 mice implanted with 005 GSCs were treated intratumorally with PBS or G47Δ-mIL2 on day 22. On day 29, mice were sacrificed, brains removed and fixed in 10% formalin, embedded in paraffin, and 5 μm sections subjected to immunohistochemical (IHC) staining for CD3 (clone SP7), CD4 (clone 4SM95), CD8 (clone 4SM15), FoxP3 (clone FJK-16s), CD68 (polyclonal), or phospho-STAT1 (clone 58D6) as described in Saha and Rabkin.<sup>27</sup> The number of positive cells was counted from 3 to 5 fields/tumor sections (1 section/mouse) (one section/mouse). The counter was blinded to the treatments.

### Statistical analysis

Survival data were analyzed by Kaplan-Meier survival curves, and comparisons were performed by log-rank test. Flow cytometric data and immunohistochemistry counts were compared using an unpaired Student's t-test (two-tailed). P values of less than 0.05 were considered significant. All statistical analyses were performed using Prism 9 software V.9.5.1.

## RESULTS

### G47Δ-mIL2 expresses IL-2 and efficiently lyses murine 005 GSCs in vitro

We engineered an oHSV called G47Δ-mIL2 (figure 1A), armed with murine IL-2 and a mCherry fluorescent reporter, using the flip-flop HSV-BAC system,<sup>24</sup> similar to the method employed for engineering an oHSV expressing murine interleukin 12 (G47Δ-mIL12).<sup>7</sup> Following established protocols, the presence of IL-2 and mCherry insertions in G47Δ-mIL2 was initially confirmed through PCR and restriction endonuclease digestion (data not shown).<sup>24</sup>

The G47Δ-mIL2 virus must enter the mouse cancer cells to produce direct oncolysis in vitro.<sup>7</sup> However, typically, mouse cells do not exhibit a high degree of susceptibility to oHSV infection.<sup>19</sup> Thus, before assessing the

cytolytic activity of G47Δ-mIL2 in vitro, we first investigated whether G47Δ-mIL2 enters mouse 005 GSCs. For this, we treated 005 GSCs with G47Δ-mIL2 at a MOI of 1.0 or PBS for 24 hours and then imaged the cells by fluorescence microscopy. The expression of the mCherry fluorescent reporter confirmed that G47Δ-mIL2 efficiently infected mouse 005 GSCs (figure 1B).

Previous research indicated that our base G47Δ virus (oHSV without cytokine expression) is efficiently oncolytic against various cancer cell lines,<sup>17, 28</sup> including human GSCs,<sup>17, 29</sup> but produces no cytotoxic effects in noncancerous healthy cells.<sup>28</sup> Here, using an MTS cytotoxicity assay, we tested the sensitivity of mouse 005 GSCs to G47Δ-mIL2. G47Δ-mIL2 infection resulted in dose-dependent oncolysis of mouse 005 GSCs in vitro, with an IC<sub>50</sub> value of MOI 0.63 (figure 1C). This oncolytic efficiency of G47Δ-mIL2 is comparable to that of other G47Δ derivatives, such as G47Δ-Empty (no cytokine expression) or G47Δ-mIL12 (IL-12 expression), in various mouse cancer cells, including 005 GSCs.<sup>7, 30–32</sup>

Cytokines must be released from cytokine-armed oHSV-infected cancer cells to bind to IL-2 receptors on T cells and induce antitumor immunity.<sup>7</sup> To investigate whether G47Δ-mIL2 infected cells release IL-2, we treated Vero cells with G47Δ-mIL2 (or control G47Δ vector) at low MOI of 0.1, collected culture supernatant at 24 hours and 48 hours postinfection, and measured IL-2 levels by ELISA. G47Δ-mIL2 infection of Vero cells resulted in the release of IL-2 in the culture supernatant, with secretion increasing from 1224 ng/mL (24 hours) to 1527 ng/mL (48 hours). In contrast, G47Δ infection did not result in any measurable IL-2 production (figure 1D). These data are consistent with the previous study demonstrating a time-dependent release of IL-12 from G47Δ-mIL12-infected mouse 005 GSCs.<sup>7</sup>

These in vitro studies demonstrate that G47Δ-mIL2 expresses the fluorescent mCherry reporter protein, produces oncolysis against mouse brain cancer cells, and releases the encoded IL-2.

### G47Δ-mIL2 demonstrated antitumor effects in orthotopic immunocompetent mouse GBM models

To evaluate the anti-GBM efficacy of G47Δ-mIL2 in vivo, C57BL/6 mice bearing intracranially established 005 GSC-derived brain tumors received a single intratumoral injection of G47Δ-mIL2 or PBS on day 8 post-tumor implantation (figure 2A). G47Δ-mIL2 treatment resulted in a significant extension of median survival by 63% (median survival=58 days) compared with PBS (median survival=35.5 days; p=0.0027) (figure 2B). In our in vivo studies, G47Δ-Empty was not included as an additional control because of its minimal effect in the 005 model.<sup>7</sup> For example, in contrast to G47Δ-mIL2, the antitumor efficacy of G47Δ-Empty (ie, an oHSV without IL-2 expression) was modest at best, with median survival extended by 10% only (vs PBS) and apparently no antitumor immune responses were seen even after two consecutive intratumoral injections on days 8 and 12.<sup>7</sup> The stark

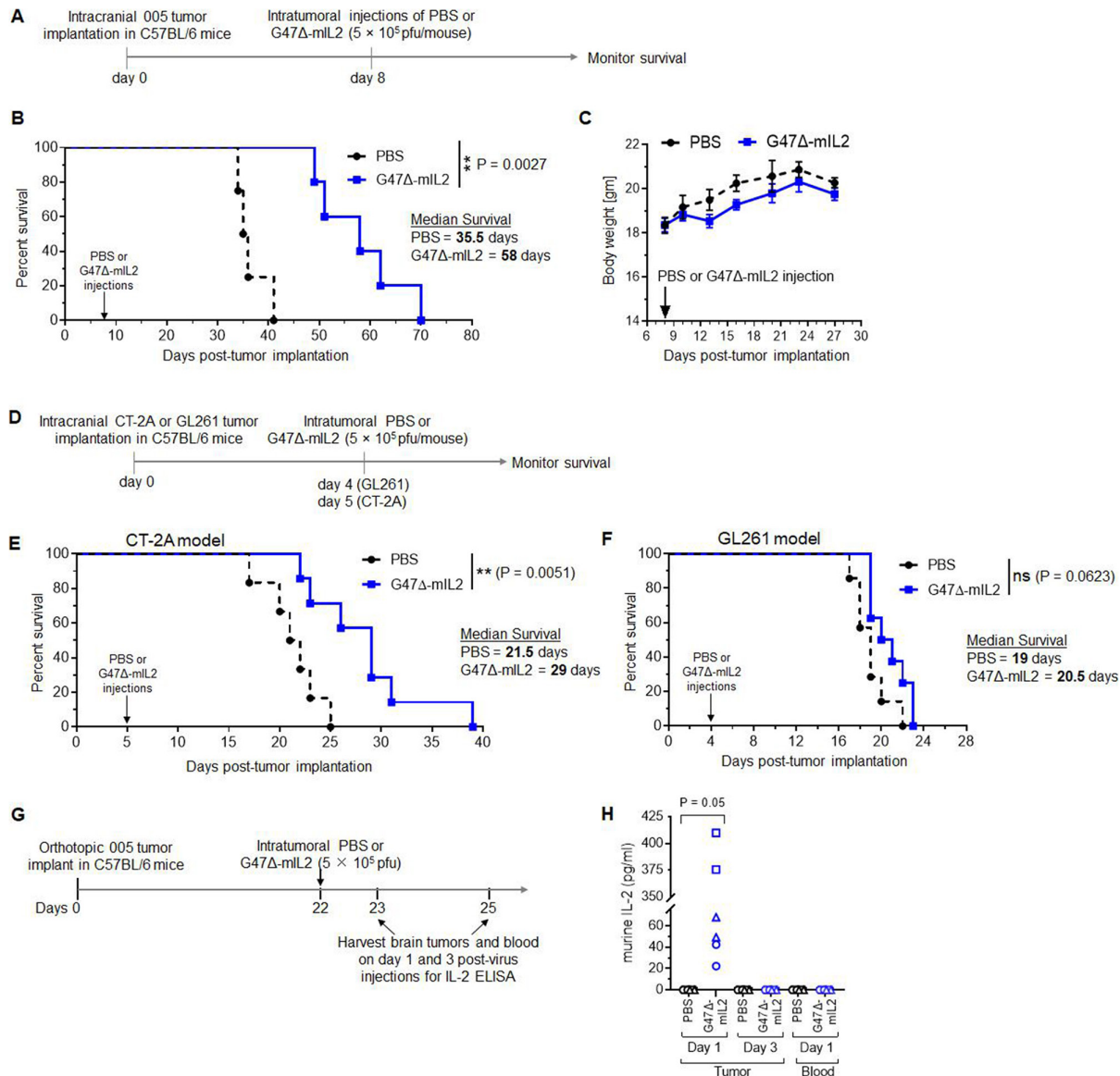


**Figure 2** (A–C) Antitumor efficacy of G47Δ-mIL2 in C57BL/6 mice bearing orthotopic mouse 005 GSC-derived brain tumors. (A) Experimental schema. C57BL/6 mice were intracranially/stereotactically implanted with mouse 005 GSCs ( $2 \times 10^4$  cells/mouse) on day 0, treated intratumorally with G47Δ-mIL2 ( $5 \times 10^5$  pfu/mouse) or PBS on day 8 ( $n=4$  for PBS and  $n=5$  for G47Δ-mIL2), and mice were followed for survival and body weights. (B) Kaplan-Meier survival curve. The median survival of the PBS group (35.5 days) is significantly different from the G47Δ-mIL2 treatment group (median survival=58 days,  $p=0.0027$ ). Log-rank (Mantel-Cox) test;  $**p<0.01$ . Note: Medium containing 005 cells came out during intracranial implantation in one mouse in the PBS group, and thus, this mouse was excluded from the study. (C) Bodyweight of tumor-bearing mice (from B) after treatment. The data are presented as mean $\pm$ SEM. No significant differences were observed between PBS and G47Δ-mIL2 treatment groups (unpaired two-tailed Student's *t*-test). (D–F) Antitumor efficacy of G47Δ-mIL2 treatment in CT-2A and GL261 GBM models. (D) Experimental schema. C57BL/6 mice intracranially/stereotactically implanted with CT-2A ( $1 \times 10^4$  cells/mouse) or GL261 cells ( $3 \times 10^4$  cells/mouse) on day 0, treated intratumorally with PBS or G47Δ-mIL2 ( $5 \times 10^5$  pfu/mouse) on day 4 (for GL261) or 5 (for CT-2A), and mice were followed for survival. (E) Kaplan-Meier survival curve in the intracranial CT-2A GBM model. The median survival time of G47Δ-mIL2 treatment (29 days;  $n=7$ ) significantly differs from the PBS group (21.5 days,  $p=0.0051$ ;  $n=6$ ). (F) Kaplan-Meier survival curve in the intracranial GL261 GBM model. The median survival time of G47Δ-mIL2 (20.5 days;  $n=8$ ) is not significantly different from the PBS group (19 days,  $p=0.0623$ ;  $n=7$ ). Log-rank (Mantel-Cox) test;  $**p<0.01$ , ns=not significant. (G–H) In vivo levels of mouse IL-2 after intratumoral treatment with G47Δ-mIL2. (G) Experimental schema. C57BL/6 mice were intracranially/stereotactically implanted with mouse 005 GSCs ( $2 \times 10^4$  cells/mouse) on day 0 and treated intratumorally with G47Δ-mIL2 ( $5 \times 10^5$  pfu/mouse) or PBS on day 22 ( $n=6$ /group). Tumor-bearing mice were euthanized on day 1 (ie, day 23,  $n=3$ /group) and 3 (ie, day 25,  $n=3$ /group) post-treatment and tumor and serum collected for IL-2 ELISA (Bio-Techne). (H) ELISA for murine IL-2 in tumor homogenates. The data show the presence of IL-2 only in the G47Δ-mIL2 treatment group on day 1. No IL-2 was detected on day 3 in the tumor homogenate or on days 1 and 3 in serum samples; thus, they were not graphed. Each animal sample was assessed in duplicate, and each shape indicates one animal (unpaired two-tailed Student's *t*-test). PBS, phosphate-buffered saline.



difference between G47Δ-Empty (10% extension vs PBS)<sup>7</sup> and G47Δ-mIL2 (63% extension vs PBS) (figure 2B) indicates the importance of IL-2 expression in vivo in mediating superior survival benefit. No neurological morbidity (data not shown) nor significant loss of body weight was noticed in the G47Δ-mIL2 treatment group (vs PBS) (figure 2C).

We also evaluated the antitumor efficacy of G47Δ-mIL2 in two additional immunocompetent orthotopic mouse GBM models, CT-2A and GL261<sup>14</sup> (figure 2D). CT-2A GBM cell-derived GBM tumors are clearly more aggressive than 005 GSC-derived GBM tumors, with a median survival of mock group being 21.5 days after intracranial implantation of  $1 \times 10^4$  CT-2A cells (figure 2E) compared with 35.5 days of median survival of mock group following intracranial implantation of  $2 \times 10^4$  005 GSCs (figure 2B). Like the CT-2A GBM model, GL261 cells are also carcinogen-induced<sup>33</sup> and similarly aggressive to CT-2A cells in forming orthotopic GBM tumors, with a median survival of PBS-treated mice 19 days following intracranial implantation of  $3 \times 10^4$  cells (figure 2F). In the CT-2A model, a single intratumoral injection of G47Δ-mIL2 resulted in a significant extension of median survival by 35% ( $p=0.0051$  vs PBS) (figure 2E), analogous to the survival advantage of G47Δ-mIL2 treatment observed in the 005 GBM model (figure 2B). However, in the GL261 model, a single intratumoral injection of G47Δ-mIL2 did not result in significant survival benefit ( $p=0.0623$  vs PBS) (figure 2F), which is likely due to the non-permissive nature of GL261 cells to oHSV infection.<sup>34 35</sup>

#### G47Δ-mIL2 releases IL-2 in vivo

We then examined if G47Δ-mIL2 treatment secreted IL-2 in vivo. C57BL/6 mice bearing established 005 GSC-derived orthotopic brain tumors were treated on day 22 post-tumor implantation with a single intratumoral injection of G47Δ-mIL2 or PBS. On days 1 and 3 post-treatment, brain tumors and serum were collected for IL-2 ELISA (Bio-Techne) (figure 2G). Murine IL-2 was detected in brain tumor homogenates on day 1 following G47Δ-mIL2 treatment but not on day 3 postvirus treatment. No IL-2 was detected in the serum, neither on day 1 nor day 3 postvirus treatment (figure 2H), indicating that secreted IL-2 remained localized within the TME.

#### G47Δ-mIL2 induces recruitment of CD8<sup>+</sup> T cells to the TME

To understand how G47Δ-mIL2 treatment extends the median survival of mice, we performed phenotyping of infiltrated cells in tumors and spleens via two complementary methods: multicolor flow cytometry staining of cells harvested from the 005 brain tumor quadrants and spleens (figure 3) and IHC staining of immune cells in the 005 brain tumors (figure 4). For flow cytometry, C57BL/6 mice bearing established 005 tumors treated with G47Δ-mIL2 or PBS on day 22 post-tumor implantation, harvested brain tumor quadrants and spleens 7 days later, processed, and subjected to flow cytometry

staining and analysis as we described<sup>10 26 32 36</sup> (see also the “Methods” section for details) (figure 3A).

At 22 days following treatment, G47Δ-mIL2 treatment did not result in any significant alteration in the percentage of GFP<sup>+</sup> 005 GSCs ( $p=0.1645$  vs PBS) while significantly increasing the percentage of CD8<sup>+</sup> T cells in the tumors ( $p=0.0301$  vs PBS) (figure 3B). Following G47Δ-mIL2 treatment, significant alteration of proliferating T cells such as CD4<sup>+</sup>Ki67<sup>+</sup> and CD8<sup>+</sup>Ki67<sup>+</sup> cells were observed in the virus-treated group compared with the PBS group (figure 3B). No significant changes were noted in the frequency of FoxP3<sup>+</sup> and PD1<sup>+</sup> subsets in T cells (figure 3B). Previous study with intratumoral G47Δ-mIL2 in the orthotopic 005 model demonstrated that cytokine expression by oHSV is localized within the tumors, resulting in no significant changes in immune cell population systemically in spleens.<sup>7</sup> Similarly, IL-2 released from intratumoral G47Δ-mIL2 treatment remained confined within the TME (figure 2H) without being detected in the peripheral circulation. Thus, as expected, probably due to the absence of systemic IL-2, G47Δ-mIL2 treatment did not result in significant changes in any tested immune cell populations systemically in spleens (figure 3C).

Similar to the flow cytometry analysis, we confirmed immune cell accumulation in the TME by IHC evaluation of different immune cell markers for T cells and macrophages in 005 brain tumor specimens. For IHC staining, we followed the same experimental/treatment schedule as the flow cytometry. Briefly, C57BL/6 mice bearing orthotopic 005 tumors received intratumoral injections of G47Δ-mIL2 or PBS on day 22 post-tumor implantation, harvested brains 7 days later (figure 4A), and formalin-fixed paraffin-embedded brain tumor sections subjected to immunochemical staining as we described<sup>9 10 27 30 32</sup> (see also the “Methods” section for details). Intratumoral G47Δ-mIL2 treatment resulted in a 2-fold increase in the number of CD8<sup>+</sup> T cells ( $p=0.0104$  vs PBS), and a 1.8-fold increase in the number of total T cells (CD3<sup>+</sup>) in the TME ( $p=0.0232$  vs PBS) (figure 4B,C). Compared with the mock-treated group, intratumoral G47Δ-mIL2 treatment did not result in any significant alteration in the number of CD4<sup>+</sup> T cells, total tumor-associated macrophages (TAMs, CD68<sup>+</sup>), and M1-like TAMs as measured by pSTAT1<sup>+</sup> cells<sup>10</sup> (figure 4B,C). Consistent with our flow cytometry data (figure 3B), IL-2 expression by G47Δ-mIL2 did not significantly increase FoxP3<sup>+</sup> Tregs within 005 tumors (figure 4C).

#### Role of immune cells in the survival efficacy of G47Δ-mIL2 treatment

IL-2 promotes the infiltration and proliferation of T cells and induces antitumor activity.<sup>21</sup> Here, we observed that viral expression of IL-2 within brain tumors is associated with increased infiltration of T cells, such as CD3<sup>+</sup> and CD8<sup>+</sup> T cells, but not macrophages into the TME (figures 3B and 4B,C). Given these observations, we wanted to confirm if T cells are responsible for the treatment efficacy seen

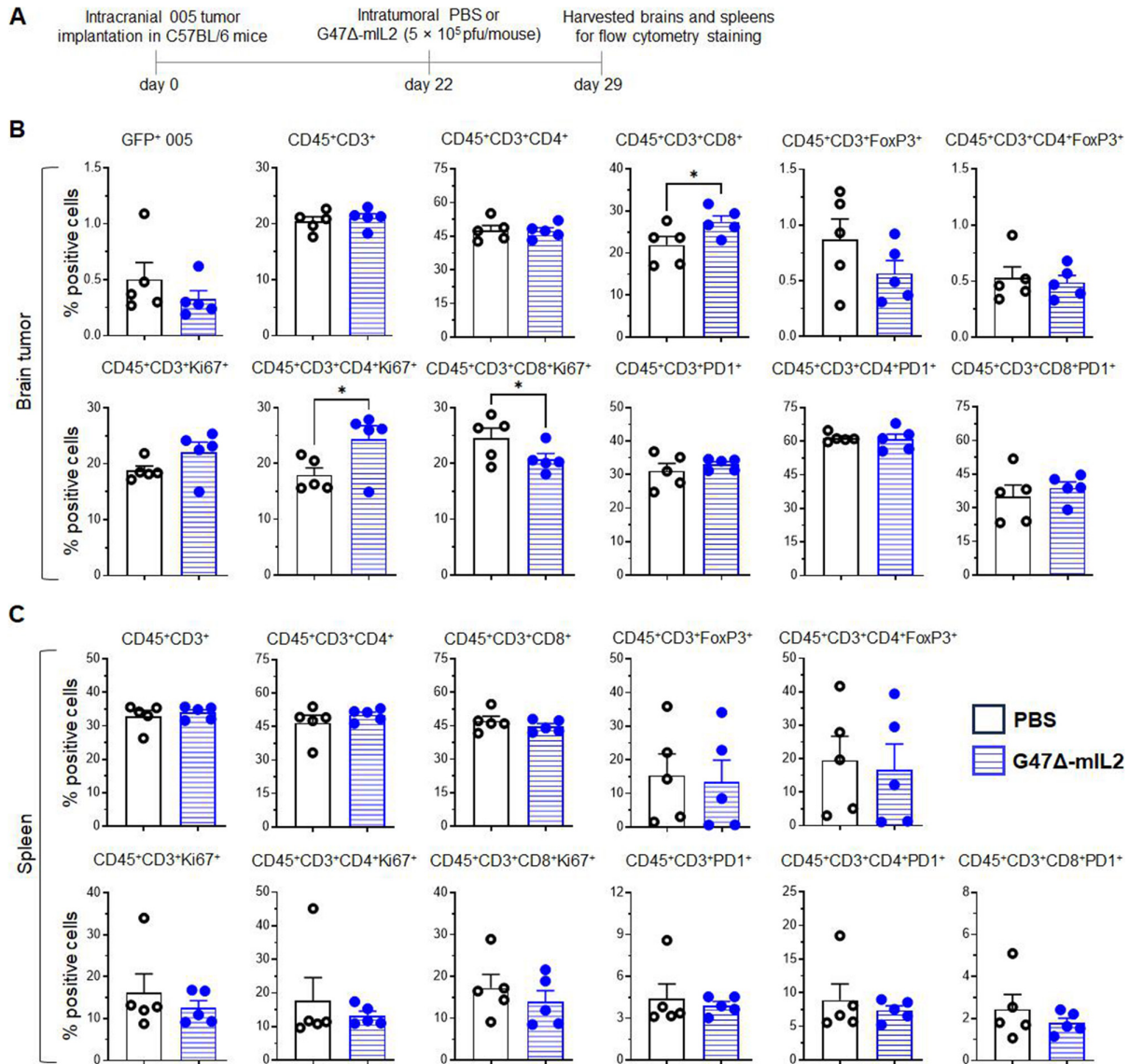


**Figure 3** Flow cytometric analysis of immune cells in 005 GSC-derived orthotopic brain tumors and spleens after G47 $\Delta$ -mIL2 treatment. (A) Experimental schema. C57BL/6 mice were intracranially/stereotactically implanted with mouse 005 GSCs ( $2 \times 10^4$  cells/mouse) on day 0, injected intratumorally with PBS ( $n=5$ ) or G47 $\Delta$ -mIL2 ( $5 \times 10^5$  pfu/mouse;  $n=5$ ) on day 22, and animals euthanized on day 29. Brains and spleens were harvested, single-cell suspensions were prepared and stained with fluorochrome-conjugated anti-mouse antibodies/dye, and multicolor fluorescence-activated cell sorting (FACS) was performed. (B, C) Bar graphs represent percentages of live sorted positive cells in brain tumors (in B) and spleens (in C). Each bullet point indicates one animal. The data are presented as mean  $\pm$  SEM. Only data that show \* $p < 0.05$  are indicated (unpaired two-tailed Student's t-test). GSC, GBM stem-like cell. PBS, phosphate-buffered saline.

in the 005 GBM model in C57BL/6 mice. For this, we first used athymic nu/nu mice (which are devoid of T cells) bearing 005 tumors, treated them with a single intratumoral injection of G47 $\Delta$ -mIL2 or PBS on day 8 post-tumor implantation, and followed mice for survival and body weights (figure 5A). Compared with the PBS group, G47 $\Delta$ -mIL2 treatment resulted in an extension of median survival by only 16% in athymic mice (figure 5B), as opposed to 63% in C57BL/6 mice (figure 2B). The reduced efficacy of G47 $\Delta$ -mIL2 in T cell-deficient athymic mice indicates the importance of T cells for G47 $\Delta$ -mIL2 treatment. Like G47 $\Delta$ -mIL2 treatment in C57BL/6 mice (figure 2C), no treatment-related toxicities nor significant

loss of body weight were observed in athymic mice after a single intratumoral injection of G47 $\Delta$ -mIL2 (vs PBS) (figure 5C).

Given the role of T cells in G47 $\Delta$ -mIL2 treatment, we then evaluated which subsets of T cells (CD4<sup>+</sup> or CD8<sup>+</sup> T cells) are essential in mediating G47 $\Delta$ -mIL2-induced survival benefit. In addition, we also tested the role of natural killer (NK) cells in the G47 $\Delta$ -mIL2-mediated treatment benefits since IL-2 enhances the cytolytic activity of NK cells.<sup>21</sup> For these purposes, C57BL/6 mice bearing intracranial 005 tumors received a single intratumoral injection of G47 $\Delta$ -mIL2 or PBS on day 8 post-tumor implantation. Simultaneously, mice received

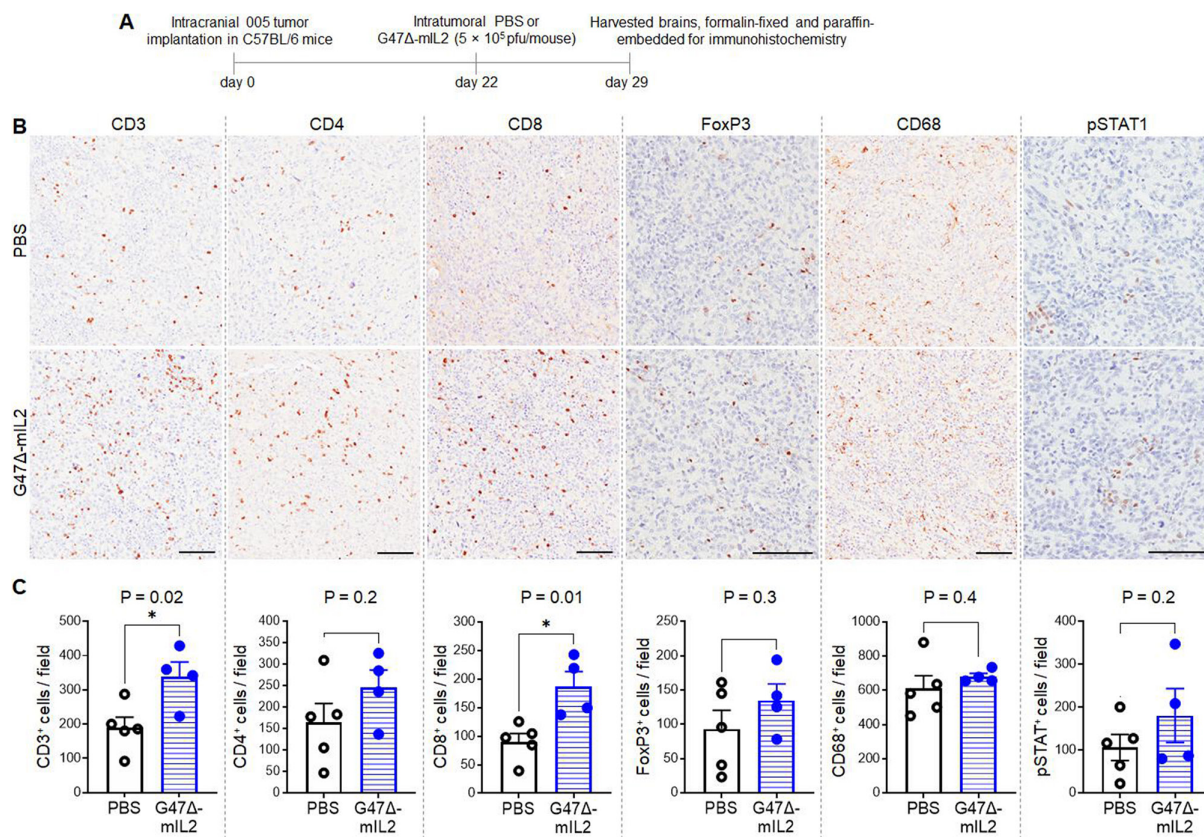


**Figure 4** Immunohistochemical staining of immune cell markers in 005 GSC-derived orthotopic brain tumors after G47Δ-mIL2 treatment. (A) Experimental schema. C57BL/6 mice were intracranially/stereotactically implanted with mouse 005 GSCs ( $3 \times 10^4$  cells/mouse) on day 0, injected intratumorally with PBS ( $n=5$ ) or G47Δ-mIL2 ( $5 \times 10^5$  pfu/mouse;  $n=4$ ) on day 22, animals euthanized on day 29, and brains harvested. (B) Formalin-fixed paraffin-embedded brain tumor sections ( $5 \mu\text{m}$  in size) were subjected to immunohistochemical staining for various mouse antigens such as CD3, CD4, CD8, FoxP3, CD68, or pSTAT1. Representative images with positive cells-stained brown are presented; scale bars= $200 \mu\text{m}$ . (C) Average number of positive cells from each individual mouse. Each bullet point represents one animal, and cells were counted from 3 to 5 fields/tumor section (one section/mouse). The mean $\pm$ SEM of all mice is presented. The statistical analysis was performed using the unpaired two-tailed Student's t-test; \* $p < 0.05$ . PBS, phosphate-buffered saline.

intraperitoneal injections of anti-CD4, anti-CD8, anti-NK1.1, anti-CD8 plus anti-NK1.1 antibodies for immune subset depletion, or control IgGs on days 4, 7, 10, 13, 20, and 27 post-tumor implantations, and followed mice for survival (figure 5D). The data presented in figure 5E show that depletion of CD4<sup>+</sup> T cells (G47Δ-mIL2 plus anti-CD4; median survival=33 days) completely abrogated the anti-GBM efficacy of G47Δ-mIL2 virus (median survival=47.5 days) to the level of mock-treated mice (median survival=35 days;  $p=0.1857$  vs G47Δ-mIL2 plus anti-CD4), indicating that the antitumor effects of G47Δ-mIL2 are fully reliant on CD4<sup>+</sup> T cells. However, infiltration of CD4<sup>+</sup> T cells in the TME (in response to G47Δ-mIL2 treatment) was not statistically significant (figures 3B and 4B,C).

In addition to CD4<sup>+</sup> T cells, CD8<sup>+</sup> T cells also play a therapeutic role since there was a significantly increased infiltration of CD8<sup>+</sup> cells into G47Δ-mIL2-treated tumors (vs PBS) (figures 3B and 4B,C). CD8<sup>+</sup> T cell depletion (G47Δ-mIL2 plus anti-CD8; median survival=38.5 days) reduced the G47Δ-mIL2-mediated survival benefit, with the borderline statistical significance of  $p=0.0505$  vs

G47Δ-mIL2 plus anti-CD8 (figure 5E). Depletion of NK1.1<sup>+</sup> cells (G47Δ-mIL2 plus anti-NK1.1; median survival=53.5 days) did not significantly affect the treatment efficacy of the G47Δ-mIL2 therapy (median survival=47.5 days;  $p=0.4451$ ) (figure 5E). However, interestingly, depletion of NK1.1<sup>+</sup> cells in the G47Δ-mIL2 plus anti-NK1.1 treatment group resulted in 2/6 long-term survivors compared with none in the G47Δ-mIL2 treatment group, implying that NK cells may have impeded the efficacy of G47Δ-mIL2 treatment.<sup>37</sup> Finally, survival was reduced with the depletion of both NK1.1<sup>+</sup> and CD8<sup>+</sup> T cells (G47Δ-mIL2 plus anti-CD8 plus anti-NK1.1; median survival=38.5 days), similar to CD8<sup>+</sup> T cell depletion, but without statistical significance ( $p=0.1075$  vs G47Δ-mIL2 plus IgG).

Overall, immune cell analysis and depletion studies (figures 3–5) indicate that both CD4<sup>+</sup> and CD8<sup>+</sup> T cells are important for the efficacy of G47Δ-mIL2 treatment, with CD4<sup>+</sup> T cells playing the key role in determining the treatment benefits of G47Δ-mIL2 virotherapy.

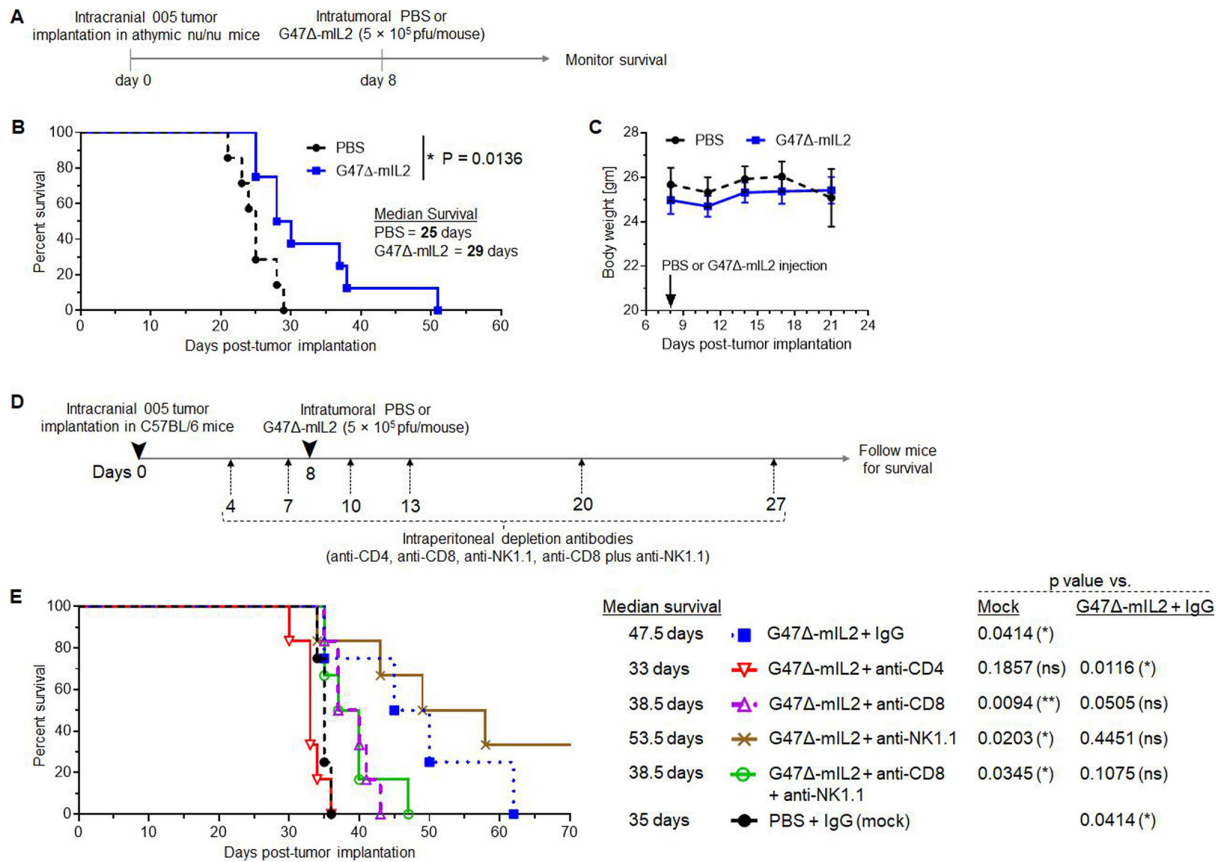


**Figure 5** (A–C) Role of T cells in G47Δ-mIL2 treatment of intracranial 005 GSC-derived brain tumors in T cell-deficient mice. (A) Experimental schema. T cell-deficient athymic nu/nu mice were intracranially/stereotactically implanted with mouse 005 GSCs ( $2 \times 10^4$  cells/mouse) on day 0, injected intratumorally with PBS ( $n=7$ ) or G47Δ-mIL2 ( $5 \times 10^5$  pfu/mouse;  $n=8$ ) on day 8, and mice were followed for survival and body weights. (B) Kaplan-Meier survival curve. The median survival of the PBS group (25 days) is significantly different from the G47Δ-mIL2 group (median survival=29 days,  $p=0.0136$ ). Log-rank (Mantel-Cox) test;  $*p<0.05$ . (C) Bodyweight of tumor-bearing mice (from B) after treatment. Mean $\pm$ SEM, no significant differences were observed between PBS and G47Δ-mIL2 treatment groups (unpaired two-tailed Student's t-test). (D, E) Role of immune cell subtypes in the treatment efficacy of G47Δ-mIL2. (D) Experimental schema. C57BL/6 mice intracranially/stereotactically implanted with mouse 005 GSCs ( $2 \times 10^4$  cells/mouse) on day 0 and treated intratumorally with PBS or G47Δ-mIL2 ( $5 \times 10^5$  pfu/mouse) on day 8. Concurrently, mice were injected intraperitoneally with anti-CD4 (clone GK1.5; 10 mg/kg), anti-CD8 (clone 2.43; 10 mg/kg), anti-NK1.1 (clone PK136; 10 mg/kg), combination of anti-CD8 plus anti-NK1.1 (10 mg/kg each), or control IgG, on days 4, 7, 10, 13, 20, and 27, and mice were followed for survival. (E) Kaplan-Meier survival curve. Median survival of mice was determined by log-rank (Mantel-Cox) test: PBS+IgG (mock;  $n=4$ ), 35 days; G47Δ-mIL2+IgG ( $n=4$ ), 47.5 days, G47Δ-mIL2+anti-CD4 ( $n=6$ ), 33 days; G47Δ-mIL2+anti-CD8 ( $n=6$ ), 38.5 days; G47Δ-mIL2+anti-NK1.1 ( $n=6$ ), 53.5 days; and G47Δ-mIL2+anti-CD8 + anti-NK1.1 ( $n=6$ ), 38.5 days. PBS+IgG (mock) was compared with G47Δ-mIL2+IgG ( $p=0.0414$ ), G47Δ-mIL2+anti-CD4 ( $p=0.1857$ ), G47Δ-mIL2+anti-CD8 (0.0094), G47Δ-mIL2+anti-NK1.1 (0.0203), or G47Δ-mIL2+anti-CD8 + anti-NK1.1 ( $p=0.0345$ ). Similarly, G47Δ-mIL2+IgG was compared with G47Δ-mIL2+anti-CD4 ( $p=0.0116$ ), G47Δ-mIL2+anti-CD8 ( $p=0.0505$ ), G47Δ-mIL2+anti-NK1.1 ( $p=0.4451$ ), G47Δ-mIL2+anti-CD8+anti-NK1.1 ( $p=0.1075$ ), or PBS+IgG ( $p=0.0414$ ). Two long-term survivors from the G47Δ-mIL2+anti-NK1.1 group were terminated on day 82, and no tumors were present. Log-rank (Mantel-Cox) test;  $*p<0.05$ ,  $**p<0.01$ , ns=not significant. Note: There were technical issues in three mice during surgeries (one from the PBS+IgG and two from the G47Δ-mIL2+IgG groups); thus, these mice were excluded from the study. GSC, GBM stem-like cell; NK, natural killer; PBS, phosphate-buffered saline.

### IL-2 expression is critical for G47Δ-mIL2-mediated therapeutic responses

Two consecutive intratumoral injections of G47Δ-Empty (no IL-2 expression) resulted in only 10% extension of median survival (vs PBS),<sup>7</sup> whereas median survival was extended by 63% with G47Δ-mIL2 treatment (vs PBS) (figure 2B). This suggests that IL-2 expression within tumors may be important for improved therapeutic activity. Based on this, we hypothesized that in vivo neutralization of IL-2 would abrogate the antitumor effects of

G47Δ-mIL2 treatment. To test this, C57BL/6 mice bearing orthotopic 005 tumors were treated intratumorally with a single intratumoral injection of G47Δ-mIL2 or PBS on day 8 post-tumor implantation. Simultaneously, to inhibit the activity of IL-2, mice received intraperitoneal injections of anti-murine(m) IL-2 or control IgG before and after virus injection, that is, on days 7, 9, 11, and 14 (figure 6A). Similar to what we observed in figure 2B G47Δ-mIL2 treatment resulted in a 76% extension of median survival ( $p=0.0029$  vs PBS) (figure 6B). However, neutralization

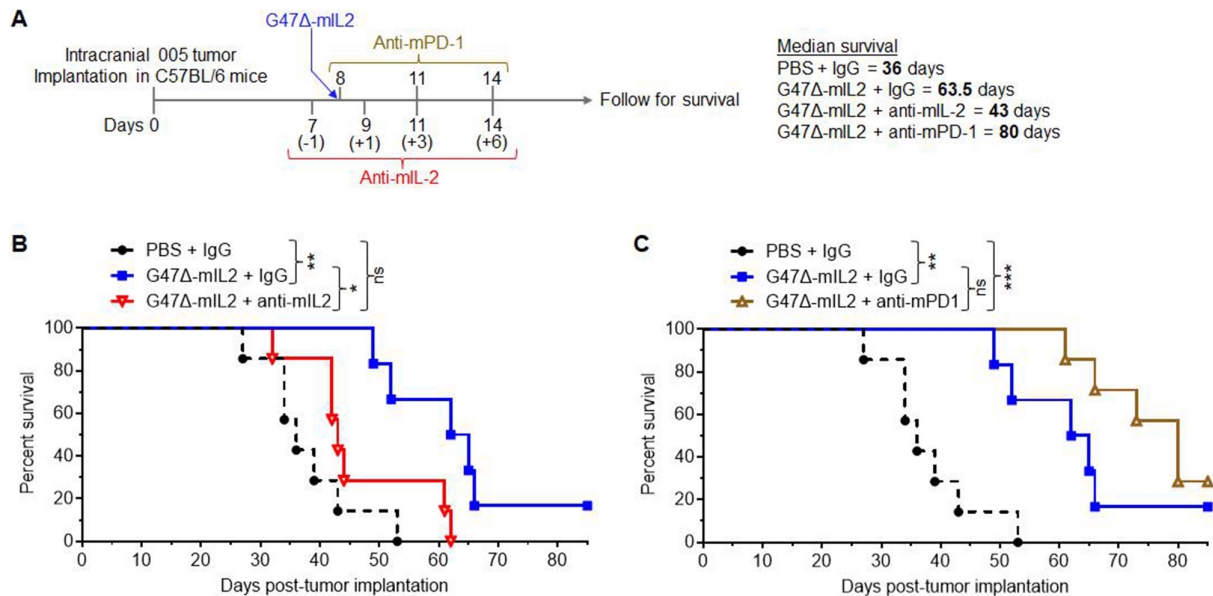


**Figure 6** Role of neutralization of IL-2 or immune checkpoint blockade in G47Δ-mIL2 treatment. (A) Experimental schema. C57BL/6 mice intracranially/stereotactically implanted with mouse 005 GSCs ( $2 \times 10^4$  cells/mouse) on day 0 and treated intratumorally with PBS or G47Δ-mIL2 ( $5 \times 10^5$  pfu/mouse) on day 8. Concurrently, mice were injected intraperitoneally with anti-murine IL-2 (anti-mIL-2) on days 7 (ie, 1 day prior to virotherapy), 9 (ie, 1 day after virus injection), 11 (ie, 3 days after virus injection), and 14 (ie, 6 days after virus injection) (clone JES6-1A12; 10 mg/kg on days 7, 9, and 11, and 7.5 mg/kg on day 14), anti-murine PD-1 (anti-mPD-1) on days 8, 11, and 14 (clone RMP1-14; 10 mg/kg), or control IgG, and mice were followed for survival. Median survival of mice was determined by Log-rank (Mantel-Cox) test: PBS+IgG (mock; n=7), 36 days; G47Δ-mIL2+IgG (n=6), 63.5 days, G47Δ-mIL2+anti-mIL-2 (n=7), 43 days, and G47Δ-mIL2+anti-mPD-1 (n=7), 80 days. Virus solution came out during intracranial injections in three mice (two from the G47Δ-mIL2+IgG and one from the G47Δ-mIL2+anti-mPD-1 groups); thus, these mice were excluded from the study. (B) Neutralization of IL-2 abrogates antitumor efficacy of G47Δ-mIL2 treatment. G47Δ-mIL2+IgG is significantly different from G47Δ-mIL2+anti-mIL-2 ( $p=0.0149$ ) or PBS+IgG ( $p=0.0029$ ), but IL-2 neutralization (ie, G47Δ-mIL2+anti-mIL-2) is not significantly different from PBS+IgG ( $p=0.1062$ ). (C) Immune checkpoint blockade (anti-mPD-1) somewhat improves the antitumor efficacy of G47Δ-mIL2 treatment. G47Δ-mIL2+anti-mPD-1 is significantly different from PBS+IgG ( $p=0.0001$ ). Although G47Δ-mIL2+anti-mPD-1 extends the median survival of mice (80 days) compared with that of G47Δ-mIL2+IgG (63.5 days), this extension is not statistically significant ( $p=0.1539$ ). In (B, C) the values are from a single experiment, with PBS+IgG and G47Δ-mIL2+IgG groups being the same in B and C. Three long-term survivors (one from G47Δ-mIL2+IgG and two from G47Δ-mIL2+anti-mPD-1 groups) were terminated on day 100, and no tumors were present. Log-rank (Mantel-Cox) test; \* $p<0.05$ , \*\* $p<0.01$ , \*\*\* $p<0.001$ , ns=not significant. PBS, phosphate-buffered saline.

of IL-2 abrogated the antitumor efficacy of G47Δ-mIL2 to the level of the mock group ( $p=0.1062$  for mock vs G47Δ-mIL2 plus anti-mIL2) (figure 6B), confirming the role of local IL-2 expression in the G47Δ-mIL2 treatment-mediated antitumor effect.

IL-2 induces T cell exhaustion by enhancing the expression of the PD-1 immune checkpoint exhaustion marker on T cells<sup>38</sup> and may compromise the efficacy of the G47Δ-mIL2 virotherapy. Thus, we evaluated if anti-PD-1 improves the activity of G47Δ-mIL2 treatment. Mice received intraperitoneal injections of anti-murine(m) PD-1 on days 8, 11, and 14 (figure 6A). We observed that the combination therapy (G47Δ-mIL2 plus anti-PD-1) further enhanced the median survival of G47Δ-mIL2 treatment by 26% (ie, the median survival increased from 63.5 days for G47Δ-mIL2 plus IgG to 80 days for G47Δ-mIL2 plus anti-PD-1); however, this improvement was not statistically significant ( $p=0.1539$ ; G47Δ-mIL2 plus anti-PD-1 vs G47Δ-mIL2 plus IgG) (figure 6C).

## DISCUSSION

Numerous preclinical studies with IL-2 armed viral vectors, such as adenoviruses, vaccinia viruses, Newcastle disease viruses, Sendai viruses, parvoviruses, tanapoxviruses, and HSV, have illustrated the effective local delivery of IL-2 to the TME, with encouraging anti-tumor outcomes while maintaining safety.<sup>22</sup> Oncolytic HSVs offer great potential for GBM treatment through both direct cytotoxic effects and immune-stimulating mechanisms.<sup>39</sup> Several genetically engineered oHSVs have been tested or are undergoing trials in GBM patients, demonstrating safety following direct inoculation into human brain.<sup>39</sup> Recently, oHSV G47Δ received approval in Japan for GBM treatment.<sup>20</sup> Arming oHSV with cytokines, such as IL-2,<sup>40 41</sup> demonstrated efficacy in mouse models.<sup>22</sup> Yet, none of these studies tested IL-2-armed oHSV, specifically in GBM or GSC-derived GBM models.

The multifaceted characteristics of IL-2, such as stimulation of T cell growth and coordinating CTL-driven antitumor responses, establish IL-2 as a pivotal proinflammatory and anticancer cytokine.<sup>21 42 43</sup> Notably, it

holds the distinction of being the first FDA-approved cytokine for cancer treatment among all interleukins.<sup>44</sup> IL-2 cytokine therapy for cancer requires frequent high-dose administration, which leads to adverse systemic events.<sup>23</sup> Conversely, low doses might compromise IL-2's anticancer effectiveness<sup>23</sup> and may also preferentially foster Treg expansion,<sup>45</sup> an undesirable outcome in cancer immunotherapy. Despite attempts to enhance safety through different delivery methods, altered dosing, binding affinity modifications, and combinations with fusion proteins, the safety of IL-2 cytokine therapy has seen only marginal improvements.<sup>46–48</sup>

OHSVs offer an effective means for targeted delivery and expression of cytokine like IL-2 within the TME. Their specificity toward tumors and capacity to trigger a controlled antitumor adaptive immune response aligns well with the amplifying immunostimulatory effects of IL-2. Here, we evaluated the antitumor effects of oHSV expressing IL-2 (G47Δ-mIL2) in mouse GBM models, including the mouse 005 GSC-derived GBM model. Previous studies demonstrated that G47Δ-mIL12 (an oHSV expressing IL-12) efficiently kills mouse 005 GSCs in vitro, with an IC50 of MOI 0.7.<sup>30–32</sup> One study also indicated the time-dependent release of cytokine from the oHSV-infected cells.<sup>7</sup> Similarly, our investigation illustrated that the newly developed G47Δ-mIL2 virus efficiently enters (as evidenced by mCherry expression) and kills mouse 005 GSCs in vitro, with an IC50 of MOI~0.67. We also observed a time-dependent release of IL-2 from G47Δ-mIL2-infected cells. Furthermore, the overall viral entry and the cytolytic activity of G47Δ-mIL2 remain comparable to other G47Δ derivatives, such as G47Δ-mCherry (expressing mCherry only) or G47Δ-Empty (lacking transgene expression), respectively.<sup>7</sup> This suggests that the expression of both transgenes, mCherry plus murine IL-2, by the G47Δ-mIL2 virus, does not negatively impact viral entry, replication, or cytotoxicity.

Mouse cancer cells exhibit lower susceptibility to oHSV infection in comparison to human cancer cells.<sup>19</sup> However, G47Δ derivatives, such as G47Δ-Empty or G47Δ-mIL12, can infect and replicate within 005 GSCs in vitro.<sup>7</sup> Notably, two consecutive intratumoral/intracranial injections of G47Δ-mIL12 into the 005 tumors lead to the intratumoral release of IL-12, indicating in vivo oHSV infection.<sup>7</sup> The viral replication increases from day 1 to day 2 postinfection and decreases by day 3.<sup>7</sup> Likewise, our newly constructed G47Δ-mIL2, following a single intratumoral/intracranial injection into the 005 tumors, also resulted in IL-2 release within the TME, indicating in vivo infection. Importantly, we observed that IL-2 secretion following G47Δ-mIL2 injection remained confined within the TME by day 1 postinfection, with no detectable IL-2 in the serum on days 1 and 3 postinfection. This absence of IL-2 in the systemic circulation after G47Δ-mIL2 treatment is vital in avoiding systemic IL-2-related adverse events. Notably, our study confirms the safety nature of G47Δ-mIL2 since we found no significant changes in the

body weights of mice following G47Δ-mIL2 treatment when compared with the PBS-treated group.

The replication of G47Δ-mIL2 and subsequent IL-2 release in the TME likely contributed to extending median survival by 63% (compared with the PBS group) in the 005 GBM model. Indeed, we confirmed the essential role of in vivo IL-2 expression for G47Δ-mIL2-mediated antitumor efficacy. We achieved this by administering intraperitoneal injections of neutralizing antibodies against IL-2 before and after G47Δ-mIL2 treatment, resulting in the nullification of G47Δ-mIL2's antitumor efficacy to a level similar to the PBS-treated group. These support a role for IL-2 expression in the antitumor effects observed in the 005 GBM model, where in previous studies, G47Δ-Empty (lacking cytokine expression) showed limited efficacy, providing only a 10% extension in median survival compared with the PBS group.<sup>7</sup>

Mouse CT-2A cells somewhat support oHSV replication, as demonstrated previously.<sup>35</sup> Similar to the observed G47Δ-mIL2-mediated survival advantage in the 005 GBM model, as anticipated, we were able to replicate to some extent the antitumor effectiveness of G47Δ-mIL2 treatment in a secondary orthotopic mouse CT-2A GBM model. In contrast to both the 005 and CT-2A GBM cells, GL261 GBM cells are non-permissive to oHSV infection.<sup>34–35</sup> Consequently, G47Δ-mIL2 treatment remains ineffective against orthotopic GL261 tumors in vivo.

The GBM TME is often described as lacking immune activity or termed as an immunologically deserted field.<sup>49</sup> Prior studies indicate that increased levels of T cells infiltrating the GBM TME, such as CD8<sup>+</sup> T cells, correlate with decreased recurrence rates and prolonged survival in GBM patients.<sup>50–51</sup> Like IL-12, IL-2 is a major anticancer cytokine that can drive T-cell proliferation and cytotoxicity.<sup>22–52</sup> More specifically, IL-2 drives the proliferation and cytotoxic activity of T cells, whereas IL-12 further skews T-cells toward cytolytic phenotype by inducing IFN-γ production.<sup>22–52</sup> Despite these differences, the survival benefit of oHSV expression of IL-12 (G47Δ-mIL12) is quite similar to that of oHSV expression of IL-2 (G47Δ-mIL2) (figure 2B)<sup>7</sup> and is associated with increased infiltration of T cells to the 005 tumors.<sup>10</sup> Similarly, here, we demonstrated that the G47Δ-mIL2 treatment-mediated survival advantage in the 005 GBM model was associated with a significantly increased infiltration of CD8<sup>+</sup> T cells, not CD4<sup>+</sup> T cells or macrophages, in the TME. IL-2 is known to drive expansion of both CD4<sup>+</sup> and CD8<sup>+</sup> T cell populations.<sup>22</sup> Interestingly, immune cell depletion studies revealed that the antitumor efficacy of G47Δ-mIL2 treatment was dependent on CD4<sup>+</sup> T cells and, to a lesser extent, on CD8<sup>+</sup> T cells. Murine 005 GSCs lack expression of both MHC class I and MHC class II (data not shown); however, IFNγ stimulation leads to induction of MHC class I expression only,<sup>7</sup> indicating CD8<sup>+</sup> T cells are more likely to be involved in mediating direct killing effects. Similar to G47Δ-mIL2 treatment in the 005 GBM model, the antitumor efficacy of G47Δ-mIL12 plus dual checkpoint inhibitors was also



completely lost in the absence of CD4<sup>+</sup> T cells.<sup>10</sup> Although we cannot rule out a direct killing role of CD4<sup>+</sup> T cells, the CD4-dependent efficacy of virotherapy in this model and lack of MHC class II expression by 005 GSCs seem to indicate that CD4<sup>+</sup> T cells are indirectly involved in priming a CD8<sup>+</sup> T cell anti-GBM response following G47Δ-mIL2 treatment. Additionally, an increasing body of research outlines the destruction of tumors facilitated by CD4<sup>+</sup> T cells, which involves the indirect elimination of MHC II-deficient tumor cells and the cytokine activity of CD4<sup>+</sup> cells.<sup>53</sup> In addition, in our prior study with G47Δ-mIL12 plus dual checkpoint inhibitor treatment in the 005 GBM model,<sup>10</sup> we demonstrated that depletion of CD4<sup>+</sup> T cells leads to a large change in proportions of other immune cells, such as CD8<sup>+</sup> T cells, in the 005 tumors,<sup>10</sup> indicating the interaction of CD4<sup>+</sup> T cells with other immune cell types in mediating the survival benefit. Future research could aim at defining the local cytokine profile and/or other immune cells in the presence and absence of CD4<sup>+</sup> T cells to elucidate their role in G47Δ-mIL2 treatment of GBM.

Prior studies demonstrated that mice devoid of NK cell cytotoxicity receptors have increased oHSV titers with an improved oHSV efficacy against GBM,<sup>37</sup> suggesting that the presence of NK cells impedes oHSV therapy in GBM. Similarly, in [figure 5E](#), the depletion of NK cells appeared to improve the efficacy of G47Δ-mIL2 treatment, with 33% of mice surviving 70 days, although this was not statistically significant (vs G47Δ-mIL2 treatment alone). However, like the published evidence,<sup>37</sup> our finding with the depletion of NK cells suggests that NK cells may have played some role in determining the anti-GBM efficacy of G47Δ-mIL2 treatment in the 005 GBM model. Like elucidating the role of CD4<sup>+</sup> T cells in G47Δ-mIL2 treatment of GBM, future research could also aim at understanding the role of NK cells in G47Δ-mIL2 replication and IL-2 expression.

One of the major drawbacks of viral expression of IL-2 is that IL-2 can enhance the expansion of Tregs, an unwanted scenario in cancer immunotherapy.<sup>45</sup> Interestingly, G47Δ-mIL2 treatment did not produce a significant effect on the infiltration of FoxP3<sup>+</sup> Tregs into 005 tumors. This could be attributed to G47Δ, the backbone of the G47Δ-mIL2 virus, which negatively impacts Treg recruitment<sup>7</sup> and may have potentially mitigated IL-2's ability to stimulate the expansion of Tregs within the tumors. Another shortcoming of IL-2 expression is that it can induce the expression of PD-1, an exhaustion marker, on T cells.<sup>38</sup> However, our data indicate that G47Δ-mIL2 treatment did not notably upregulate PD-1 expression on the analyzed T cell subsets in the tumors and spleens. Consequently, anti-PD-1 immune checkpoint blockade did not significantly enhance the survival advantage provided by G47Δ-mIL2 treatment.

In summary, we show for the first time that oHSV expression of IL-2 (G47Δ-mIL2) is effective in improving the median survival of mice bearing orthotopic GBM tumors, including those composed of GSCs, without producing

any observable toxicities. Mechanistically, T cells, especially CD4<sup>+</sup> T cells, are the key cellular mediators associated with G47Δ-mIL2-induced therapeutic responses in GBM. The data suggest that G47Δ-mIL2 may mediate antitumor activity against GBM with minimal systemic toxicity. Considering the safety profile of other oHSVs in development for GBM treatment,<sup>39</sup> our findings provide the rationale for translating G47Δ-IL2 into the clinic for evaluation in patients with GBM.

**Acknowledgements** We thank Dr. I. Verma (Salk Institute, San Diego, CA) for providing the 005 GSCs, Dr. T. Seyfried (Boston College, MA) for the CT-2A cells, and the Division of Cancer Treatment and Diagnosis (DCTD) Tumor Repository, Biological Testing Branch (BTB) at the National Cancer Institute (NCI) for the GL261 cells. We also sincerely acknowledge the following individuals for their technical help: Ms. Humphrey for her technical assistance during virus construction, Ms. Guzmontgomery for her technical help during intracranial mouse surgeries, preparing paraffin blocks and taking care of mice, Ms. Nguyen for her technical help with the Aperio Digital Slide Scanner, and all personnel at the Laboratory Animal Resource Center at TTUHSC-Abilene for their overall supervision of mice used in this study and members of the Brain Tumor Research Center at Massachusetts General Hospital for their support.

**Contributors** DS: conceptualized the study and study design, performed in vitro (assisted with virus construction) and in vivo studies (mouse surgeries, flow cytometry, immunohistochemistry), data analysis, wrote the manuscript, and funding; PKB: conceptualized, constructed, and characterized the G47Δ-mIL2 virus in vitro; HW: provided technical guidance and reagents; RLM: provided financial support and guidance; HLK: conceptualized the idea to generate G47Δ-mIL2 virus and provided clinical perspective; SDR: provided overall guidance and financial support and performed data analysis. All authors contributed to the editing of the manuscript and approved the submitted version. Guarantor author: DS.

**Funding** DS was supported in part by a grant from the DOD (W81XWH-20-1-0702) and startup funds from Dodge Jones Foundation-Abilene and TTUHSC-School of Pharmacy. The research was funded in part by grants from NIH (R01 CA160762 to SDR and R01 NS032677 to RLM). PKB was supported by the special study award from the Rutgers School of Graduate Studies and The Cancer Institute of New Jersey.

**Competing interests** SDR and RLM are coinventors on patents relating to oncolytic herpes simplex viruses, owned and managed by Georgetown University and Massachusetts General Hospital, which have received royalties from Amgen and ActiVec. SDR acted as consultant and received honoraria from Replimune and honoraria and equity from EG 427. PKB is currently an employee of Replimune Inc. HLK is an employee of Ankyra Therapeutics and has received honoraria for participating on advisory boards for Castle Biosciences, Midatech Pharma, Marengo Therapeutics, and Virogin. The remaining authors declare that the research was conducted in the absence of any commercial or financial relationships that could be construed as a potential conflict of interest.

**Patient consent for publication** Not applicable.

**Ethics approval** All mouse procedures were approved by the Institutional Animal Care and Use Committee at TTUHSC (IACUC protocols #18033 and 19183).

**Provenance and peer review** Not commissioned; externally peer reviewed.

**Data availability statement** Data are available on reasonable request. All data relevant to the study are included in the article.

**Open access** This is an open access article distributed in accordance with the Creative Commons Attribution Non Commercial (CC BY-NC 4.0) license, which permits others to distribute, remix, adapt, build upon this work non-commercially, and license their derivative works on different terms, provided the original work is properly cited, appropriate credit is given, any changes made indicated, and the use is non-commercial. See <http://creativecommons.org/licenses/by-nc/4.0/>.

#### ORCID iDs

Praveen K Bommareddy <http://orcid.org/0000-0003-0089-8693>  
 Hiroaki Wakimoto <http://orcid.org/0000-0001-8225-241X>  
 Howard L Kaufman <http://orcid.org/0000-0003-1131-004X>  
 Samuel D Rabkin <http://orcid.org/0000-0003-2344-2795>  
 Dipongkor Saha <http://orcid.org/0000-0002-9923-5533>

## REFERENCES

- 1 Nguyen H-M, Guz-Montgomery K, Lowe DB, et al. Pathogenetic features and current management of glioblastoma. *Cancers (Basel)* 2021;13:856.
- 2 Reardon DA, Brandes AA, Omuro A, et al. Effect of nivolumab vs bevacizumab in patients with recurrent glioblastoma: the checkmate 143 phase 3 randomized clinical trial. *JAMA Oncol* 2020;6:1003–10.
- 3 Dirkse A, Golebiewska A, Buder T, et al. Stem cell-associated heterogeneity in glioblastoma results from intrinsic tumor plasticity shaped by the microenvironment. *Nat Commun* 2019;10:1787.
- 4 Dirks PB. Brain tumor stem cells: the cancer stem cell hypothesis writ large. *Mol Oncol* 2010;4:420–30.
- 5 Lee J, Kotliarova S, Kotliarov Y, et al. Tumor stem cells derived from glioblastomas cultured in bFGF and EGF more closely mirror the phenotype and genotype of primary tumors than do serum-cultured cell lines. *Cancer Cell* 2006;9:391–403.
- 6 Wakimoto H, Mohapatra G, Kanai R, et al. Maintenance of primary tumor phenotype and genotype in glioblastoma stem cells. *Neuro Oncol* 2012;14:132–44.
- 7 Cheema TA, Wakimoto H, Fecci PE, et al. Multifaceted oncolytic virus therapy for glioblastoma in an immunocompetent cancer stem cell model. *Proc Natl Acad Sci U S A* 2013;110:12006–11.
- 8 Marumoto T, Tashiro A, Friedmann-Morvinski D, et al. Development of a novel mouse glioma model using lentiviral vectors. *Nat Med* 2009;15:110–6.
- 9 Saha D, Martuza RL, Rabkin SD. Oncolytic herpes simplex virus immunovirotherapy in combination with immune checkpoint blockade to treat glioblastoma. *Immunotherapy* 2018;10:779–86.
- 10 Saha D, Martuza RL, Rabkin SD. Macrophage polarization contributes to glioblastoma eradication by combination immunovirotherapy and immune checkpoint blockade. *Cancer Cell* 2017;32:253–67.
- 11 Saha D, Martuza RL, Rabkin SD. Curing glioblastoma: oncolytic HSV-II12 and checkpoint blockade. *Oncoscience* 2017;4:67–9.
- 12 Khalsa JK, Shah K. Immune profiling of syngeneic murine and patient GBMs for effective translation of Immunotherapies. *Cells* 2021;10:491.
- 13 Seyfried TN, el-Abbadi M, Ecsedy JA, et al. Influence of host cell infiltration on the glycolipid content of Mouse brain tumors. *J Neurochem* 1996;66:2026–33.
- 14 Oh T, Fakurnejad S, Sayegh ET, et al. Immunocompetent murine models for the study of glioblastoma Immunotherapy. *J Transl Med* 2014;12:107.
- 15 Riva M, Wouters R, Weerasekera A, et al. CT-2A Neurospheres-derived high-grade glioma in mice: a new model to address tumor stem cells and immunosuppression. *Biol Open* 2019;8:bio044552.
- 16 Bommareddy PK, Peters C, Saha D, et al. Oncolytic herpes simplex viruses as a paradigm for the treatment of cancer. *Annu Rev Cancer Biol* 2018;2:155–73.
- 17 Wakimoto H, Kesari S, Farrell CJ, et al. Human glioblastoma-derived cancer stem cells: establishment of invasive glioma models and treatment with oncolytic herpes simplex virus vectors. *Cancer Res* 2009;69:3472–81.
- 18 Andtbacka RHI, Kaufman HL, Collichio F, et al. Talimogene laherparepvec improves durable response rate in patients with advanced melanoma. *J Clin Oncol* 2015;33:2780–8.
- 19 Todo T, Martuza RL, Rabkin SD, et al. Oncolytic herpes simplex virus vector with enhanced MHC class I presentation and tumor cell killing. *Proc Natl Acad Sci U S A* 2001;98:6396–401.
- 20 Todo T, Ito H, Ino Y, et al. Intratumoral oncolytic herpes virus G47Δ for residual or recurrent glioblastoma: a phase 2 trial. *Nat Med* 2022;28:1630–9.
- 21 Muhammad S, Fan T, Hai Y, et al. Reigniting hope in cancer treatment: the promise and pitfalls of IL-2 and IL-2R targeting strategies. *Mol Cancer* 2023;22:121:121..
- 22 Wang H, Borlongan M, Hemminki A, et al. Viral vectors expressing interleukin 2 for cancer Immunotherapy. *Hum Gene Ther* 2023;34:878–95.
- 23 Pachella LA, Madsen LT, Dains JE. The toxicity and benefit of various dosing strategies for Interleukin-2 in metastatic melanoma and renal cell carcinoma. *J Adv Pract Oncol* 2015;6:212–21.
- 24 Kuroda T, Martuza RL, Todo T, et al. Flip-flop HSV-BAC: bacterial artificial chromosome based system for rapid generation of recombinant herpes simplex virus vectors using two independent site-specific Recombinases. *BMC Biotechnol* 2006;6:40.
- 25 Nguyen H-M, Sah N, Humphrey MRM, et al. Growth, purification, and titration of oncolytic herpes simplex virus. *J Vis Exp* May 13, 2021.
- 26 Bommareddy PK, Lowe DB, Kaufman HL, et al. Multi-parametric flow cytometry staining procedure for analyzing tumor-infiltrating immune cells following oncolytic herpes simplex virus immunotherapy in intracranial glioblastoma. *J Biol Methods* 2019;6:e112.
- 27 Saha D, Rabkin SD. Immunohistochemistry for tumor-infiltrating immune cells after oncolytic virotherapy. *Methods Mol Biol* 2020;2058:179–90.
- 28 Wang J, Hu P, Zeng M, et al. Oncolytic herpes simplex virus treatment of metastatic breast cancer. *Int J Oncol* 2012;40:757–63.
- 29 Kanai R, Rabkin SD, Yip S, et al. Oncolytic virus-mediated manipulation of DNA damage responses: synergy with chemotherapy in killing glioblastoma stem cells. *J Natl Cancer Inst* 2012;104:42–55.
- 30 Saha D, Wakimoto H, Peters CW, et al. Combinatorial effects of VEGFR kinase inhibitor axitinib and oncolytic virotherapy in mouse and human glioblastoma stem-like cell models. *Clin Cancer Res* 2018;24:3409–22.
- 31 Ghouse SM, Nguyen H-M, Bommareddy PK, et al. Oncolytic herpes simplex virus encoding II12 controls triple-negative breast cancer growth and metastasis. *Front Oncol* 2020;10:384:384..
- 32 Saha D, Rabkin SD, Martuza RL. Temozolomide antagonizes oncolytic immunovirotherapy in glioblastoma. *J Immunother Cancer* 2020;8:e000345.
- 33 Szatmári T, Lumniczky K, Désaknai S, et al. Detailed characterization of the mouse glioma 261 tumor model for experimental glioblastoma therapy. *Cancer Sci* 2006;97:546–53.
- 34 Nakashima H, Nguyen T, Kasai K, et al. Toxicity and efficacy of a novel Gadd34-expressing oncolytic HSV-1 for the treatment of experimental glioblastoma. *Clin Cancer Res* 2018;24:2574–84.
- 35 Alayo QA, Ito H, Passaro C, et al. Glioblastoma infiltration of both tumor- and virus-antigen specific cytotoxic T cells correlates with experimental virotherapy responses. *Sci Rep* 2020;10:5095.
- 36 Jahan N, Talat H, Alonso A, et al. Triple combination immunotherapy with GVAX, anti-PD-1 monoclonal antibody, and agonist anti-Ox40 monoclonal antibody is highly effective against murine intracranial glioma. *Oncimmunology* 2019;8:e1577108.
- 37 Alvarez-Breckenridge CA, Yu J, Price R, et al. NK cells impede glioblastoma virotherapy through Nkp30 and Nkp46 natural cytotoxicity receptors. *Nat Med* 2012;18:1827–34.
- 38 Kwon B. The two faces of IL-2: a key driver of Cd8<sup>+</sup> T-cell exhaustion. *Cell Mol Immunol* 2021;18:1641–3.
- 39 Kardani K, Sanchez Gil J, Rabkin SD. Oncolytic herpes simplex viruses for the treatment of glioma and targeting glioblastoma stem-like cells. *Front Cell Infect Microbiol* 2023;13:1206111.
- 40 Ravirala D, Mistretta B, Gunaratne PH, et al. Co-delivery of novel bispecific and trispecific engagers by an amplicon vector augments the therapeutic effect of an HSV-based oncolytic virotherapy. *J Immunother Cancer* 2021;9:e002454.
- 41 Carew JF, Kooby DA, Halterman MW, et al. A novel approach to cancer therapy using an oncolytic herpes virus to package amplicons containing cytokine genes. *Mol Ther* 2001;4:250–6.
- 42 Jiang T, Zhou C, Ren S. Role of IL-2 in cancer immunotherapy. *Oncimmunology* 2016;5:e1163462.
- 43 Ross SH, Cantrell DA. Signaling and function of Interleukin-2 in T lymphocytes. *Annu Rev Immunol* 2018;36:411–33.
- 44 Choudhry H, Helmi N, Abdulla WH, et al. Prospects of IL-2 in cancer immunotherapy. *Biomed Res Int* 2018;2018:9056173.
- 45 Mitra S, Leonard WJ. Biology of IL-2 and its therapeutic modulation: mechanisms and strategies. *J Leukoc Biol* 2018;103:643–55.
- 46 MacDonald A, Wu T-C, Hung C-F. Interleukin 2-based fusion proteins for the treatment of cancer. *J Immunol Res* 2021;2021:7855808.
- 47 Davey RT Jr, Chaitt DG, Piscitelli SC, et al. Subcutaneous administration of Interleukin-2 in human immunodeficiency virus type 1-infected persons. *J Infect Dis* 1997;175:781–9.
- 48 Lotze MT, Custer MC, Rosenberg SA. Intraperitoneal administration of Interleukin-2 in patients with cancer. *Arch Surg* 1986;121:1373–9.
- 49 Gershon R, Polevikov A, Karepov Y, et al. Frequencies of 4 tumor-infiltrating lymphocytes potentially predict survival in glioblastoma, an immune desert. *Neuro Oncol* 2024;26:473–87.
- 50 Mauldin IS, Jo J, Wages NA, et al. Proliferating Cd8<sup>+</sup> T cell infiltrates are associated with improved survival in glioblastoma. *Cells* 2021;10:3378.
- 51 Alanio C, Binder ZA, Chang RB, et al. Immunologic features in de novo and recurrent glioblastoma are associated with survival outcomes. *Cancer Immunol Res* 2022;10:800–10.
- 52 Nguyen H-M, Guz-Montgomery K, Saha D. Oncolytic virus encoding a master pro-inflammatory cytokine interleukin 12 in cancer Immunotherapy. *Cells* 2020;9:400.
- 53 Kruse B, Buzzati AC, Shridhar N, et al. Cd4<sup>+</sup> T cell-induced inflammatory cell death controls immune-evasive tumours. *Nature* 2023;618:1033–40.